Applied Radiation and Isotopes 114 (2016) 76–86

Contents lists available at ScienceDirect

Applied Radiation and Isotopes

journal homepage: www.elsevier.com/locate/apradiso

In situ γ-ray spectrometry in the marine environment using full spectrum analysis for natural radionuclides

E.G. Androulakaki [a,b,*], M. Kokkoris [a], C. Tsabaris [b], G. Eleftheriou [b,c], D.L. Patiris [b], F.K. Pappa [a,b], R. Vlastou [a]

[a] Department of Physics, National Technical University of Athens, Zografou, Greece
[b] Institute of Oceanography, Hellenic Centre for Marine Research, Anavyssos, Greece
[c] Department of Monitoring and Research, Norwegian Radiation Protection Authority, Norway

HIGHLIGHTS

- Full Spectrum analysis technique.
- Implementation of the MCNP-CP code for the reproduction of the 'standard spectra'.
- Rapid activity concentration estimations by performing the χ^2 minimization in properly selected windows.
- MDA values for any radionuclide in different aquatic environments.

ARTICLE INFO

Article history:
Received 23 February 2016
Received in revised form
9 May 2016
Accepted 10 May 2016
Available online 11 May 2016

Keywords:
Monte carlo simulation
MCNP-CP
Full spectrum analysis
In situ radioactivity measurements
Marine environment

ABSTRACT

The Full Spectrum Analysis approach was applied to obtain activity concentration estimations for *in situ* measurements in the marine environment. The 'standard spectra' were reproduced using the MCNP-CP code. In order to extract the activity concentrations, χ^2 minimization calculations were performed by implementing the MINUIT code. The method was applied to estimate the activity concentrations for measurements in the marine environment in three different test cases. The estimated activity concentrations were in good agreement with the experimentally derived ones within uncertainties.

1. Introduction

An increasing demand for fast measurements in the marine environment for radiological purposes is evident nowadays, due to the expansion of industrial activities and nuclear power plants near coastal areas. Among the available techniques, the *in situ* method provides a cost-effective and easy to apply technique. Moreover, the measurements are much faster compared to laboratory ones and more representative of the studied environment, since they are performed directly on the field. Therefore, the development and the implementation of *in situ* systems for measurements in the environment continuously evolve. A brief discussion on the up to date available *in situ* systems and the utilized quantification methods has been presented in the works of Hendriks et al. (2001), Jones (2001) and Povinec et al. (2008).

The most commonly used approach for the analysis of the *in situ* spectra, is to monitor broad spectral windows that include the photopeaks of the radionuclides of interest. Nevertheless, there are some important drawbacks inherent in this method, starting from the fact that only a limited spectral information is exploited, since the analysis is usually performed in three energy windows, namely around the ^{40}K (1460 keV), the ^{214}Bi (609 keV) and the ^{208}Tl (2614 keV) photopeaks. More importantly, since the majority of the available *in situ* systems consist of low resolution crystals (e.g. BGO, NaI), large uncertainties may occur in the window analysis, as for instance, the existence of convoluted peaks in the case of the triplet at 583 (^{208}Tl), 609 (^{214}Bi), and 662 (^{137}Cs) keV, or the convoluted peaks of ^{40}K, ^{214}Bi and ^{228}Ac around 1460 keV. Two additional parameters which contribute to the overall uncertainty are the different approaches utilized to remove the background counts and the low counting rates that are usually present in measurements in the marine environment. Moreover,

* Corresponding author.

http://dx.doi.org/10.1016/j.apradiso.2016.05.008
0969-8043/

the most crucial drawback is the inability of the method to identify other radionuclides (Caciolli et al., 2012) that may contribute to the count rate in the corresponding window interval. The presence of additional contributing radionuclides in one of the utilized windows would lead to erroneous results in the determination of the activity concentration values (Guillot et al., 2001).

Therefore, the window analysis has been gradually substituted by more promising methods that rely on the Full Spectrum Analysis (FSA) technique and can overcome the aforementioned disadvantages. The benefits of the utilization of the FSA technique are (a) the decrease of the acquisition time required to reach sufficient accuracy (Hendriks et al., 2001) and (b) the exploitation of the full extent of the spectrum, that offers the possibility to quantify more radionuclides, to crosscheck the results from different peaks and to detect anomalies (e.g. identify the presence of other radionuclides that were not considered in the analysis).

The FSA technique is based on producing separate standard spectra for the radionuclides of interest, either from different calibration measurements (Caciolli et al., 2012; Hendriks et al., 2001), or by MC simulations (van der Graaf et al., 2011; Vlastou et al., 2006; Maučec et al., 2004), taking into account the exact geometry and features of the actual *in situ* measurement. The spectrum of the actual measurement is represented by a linear combination of the standard spectra multiplied by the corresponding activity concentration values for each radionuclide, which are the unknown parameters that need to be calculated. The optimal activity concentrations are derived by fitting the simulated spectrum to the measured one, using different numerical methods to perform the minimization procedure and reach convergence.

During the last decade, techniques based on FSA have been implemented, for various *in situ* detection systems in different applications. Quantitative data for measurements in soils (Mahmood et al., 2013; Caciolli et al., 2012; van der Graaf et al., 2011), sediments (Maučec et al., 2004) and airborne studies (Guillot et al., 2001; Hendriks et al., 2001; Minty et al., 1992) have already been obtained. Nevertheless, the available methodologies consider a minimum number of radionuclides and in some cases assume that the secular equilibrium is secured for the natural radionuclides under study of the same series. A FSA technique that considers all the prominent radionuclides present in the environment without *a priori* assuming secular equilibrium has been implemented in the aquatic environment in the past (Vlastou et al., 2006), but due to the adopted approach yielded only qualitative results.

In the present work, a method using the FSA technique has been developed, able to provide rapid estimations of activity concentrations for *in situ* measurements in the aquatic environment using a low resolution detector. The MCNP-CP code (Berlizov, 2006) is implemented to derive the 'standard spectra'. The optimal activity concentration values were derived by reproducing the actual spectrum using a linear combination of the standard spectra, bearing different normalization factors as fitting parameters. The fitting procedure was performed via χ^2minimization using the MINUIT code developed at CERN. The method was initially tested in the laboratory, using reference spectra acquired in a water tank containing diluted ^{40}K, ^{99m}Tc and ^{137}Cs sources of known activity concentrations. Subsequently, the method was applied to derive the activity concentrations in three *in situ* measurements performed in different marine environments (NE Mediterranean). The theoretically estimated values are compared with the corresponding experimental results. Aspects of the optimization of the method as well as future applications are discussed.

2. Methodology description

2.1. MC simulations

The MC method is a powerful auxiliary tool suitable for simulations of particle transport, especially in complex-geometry, multi-layer problems and thus, is widely implemented for detection efficiency calculations in various areas of applied nuclear and particle physics, as well as in FSA applications (Wang et al., 2015; Berlizov and Mayer, 2010; Vlastou et al., 2006). In the present work the MCNP-CP code is implemented for the reproduction of the required standard spectra (Jäderström et al., 2015), instead of utilizing calibration spectra obtained *in situ* (Caciolli et al., 2012) or using reference sources (Hendriks et al., 2001).

The MCNP-CP code is an extended version of the general purpose Monte-Carlo N-Particle transport code MCNP4c (Briesmeister, 1997) and is a validated code which reproduces experimental data for various applications (Szentmiklósi et. al., 2013; Berlizov et. al. 2011; Zhu et. al. 2008), including environmental ones (Jäderström et al., 2015; Berlizov and Mayer, 2010; Berlizov and Solovyena, 2008). The great benefit of the utilized MC code is its ability to incorporate in the simulations a source of correlated nuclear particles based on the Evaluated Nuclear Structure Data File (ENSDF). The direct simulation of all the prominent emitted γ-rays (exhibiting an emission probability $>0.3\%$) along with the corresponding intensities for each radionuclide is achieved via a single command card (ZAM option, extension of the SDEF card). Therefore, each standard spectrum is accurately and efficiently reproduced, consisting of all the emitted γ-rays and taking into account the corresponding intensity probabilities for each single radionuclide present in the marine environment. Moreover, using this code more than one photon per event can be generated and simultaneously transported in every step of the simulation and therefore offers the possibility to account for true coincidence-summing (TCS) effects using again a single card (Correlated Particle Source settings card CPS). Both of the aforementioned advantages are critical for applications in the marine environment, since the measurements are performed in contact geometries between the source and the detector and therefore TCS effects for cascade radionuclides are always present. Moreover numerous radionuclides with complicated decay schemes contribute to the measurements and therefore an efficient simulation of all the corresponding emitted γ-rays is necessary.

The reproduction of the standard spectra was assessed using the pulse-height estimator, F8 tally (X-5 Monte Carlo Team, 2003), which gives the pulses per initial event recorded in an energy window selected by the user. A histogram over an energy window ranging from 0 keV to 3000 keV, with an 1 keV binning step, was generated. The small energy binning enhances the accuracy of the obtained results as compared to van der Graaf et al. (2011), at the expense of computing time necessary to reduce the statistical error per bin. Nevertheless, it should be noted here that the generation of the MC histograms for all radionuclides is carried out only once, since the simulation of the electronic setup and detector resolution effects is assessed via external algorithms and not through the MC code. The geometry and the materials of the experimental measurement were carefully introduced in the simulations. The simulated geometrical setup (Androulakaki et al., 2015) is shown in Fig. 1.

The 'infinite' geometry of the measurement is represented in the simulation by an extended water source having the shape of a sphere (Androulakaki et al., 2015; Zhang et al., 2015), and denoted hereafter in the document as the 'effective volume', in which the photons are generated. The effective radius of the sphere was calculated using the Beer-Lambert law (exponential attenuation law). The utilized total attenuation coefficients were derived from

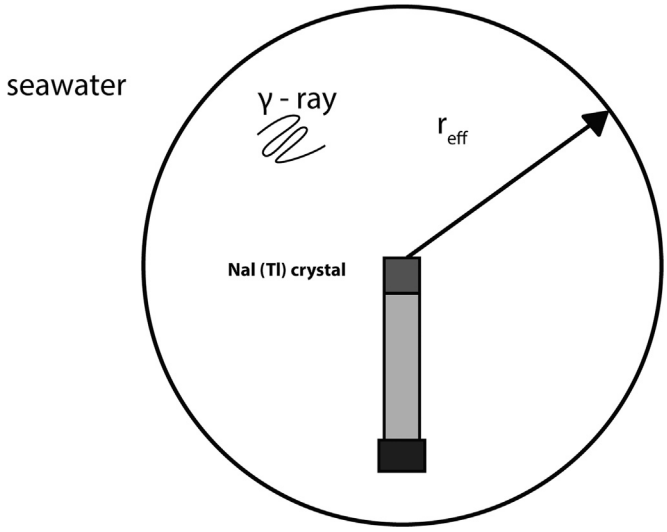

Fig. 1. Schematics of the measurement setup in the marine environment (Androulakaki et al., 2015).

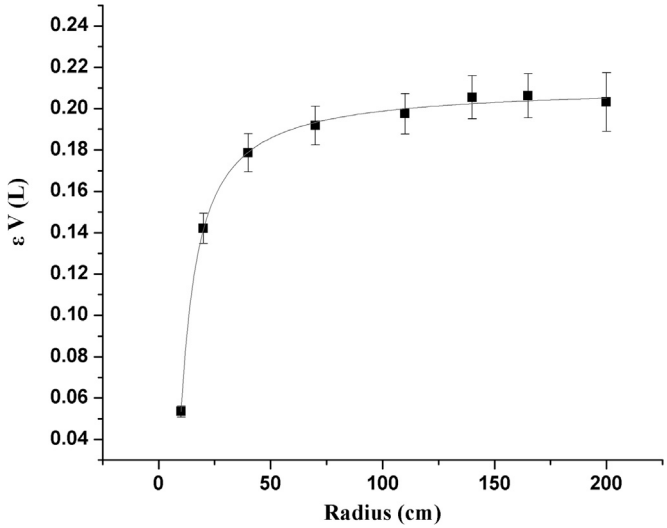

Fig. 2. Schematics of the effect of the source radius to the detection efficiency ($\varepsilon \cdot V$) of photons from ^{208}Tl having an energy of 583 keV.

the software X-COM (Berger et al., 2010) at different energies. However, since each radionuclide is simulated as a whole, taking into account all the emitted γ-rays, only one proper single effective volume had to be defined. This obstacle of selecting the proper dimensions of the sphere representing the source was overcome considering the following argument. The volumetric detection efficiency ($\varepsilon \cdot V$) is the product of the volume of the source (V) and the full-energy peak efficiency (ε), provided from the MC output (F8 tally). If the volume of the source is larger than the effective one but the number of generated events per units of volume (N/V) remains constant, the volumetric detection efficiency does not change. This has been confirmed elsewhere via different MC codes (Zhang et al., 2015; Bagatelas et al., 2010) and also in this work for the case of ^{208}Tl at 583 keV. As shown in Fig. 2, the volumetric detection efficiency ($\varepsilon \cdot V$) reaches a plateau around the effective radius and remains constant even if the radius is further increased. This is a reasonable result, since, by definition, the photons generated outside the effective volume cannot reach the detector. Therefore, in each standard spectrum, the spherical volume representing the source (effective volume) was calculated with respect to the γ-ray with the highest energy.

The raw MC results represent the full-energy peak efficiency, **ε**, as a function of energy and are by default normalized for the emission probability of each γ-ray for each radionuclide. Nevertheless, additional calculations are needed to convert the MC results to spectra (counts per channels). Therefore, the raw MC results for each radionuclide were multiplied with the corresponding effective volume, V_{eff}, and with the experimental acquisition time, T. The additional quantity that should be multiplied in order to convert the MC results in counts per channels is the activity concentration (in untis of Bq/l) of each radionuclide. This quantity is the unknown parameter (α_j) that is determined through χ^2 minimization.

The naturally occurring radionuclides present in the marine environment, namely ^{208}Tl, ^{228}Ac, ^{212}Bi, ^{212}Pb (series of ^{232}Th), ^{214}Bi, ^{214}Pb, ^{234}Pa, ^{226}Ra, ^{222}Rn (series of ^{238}U) and ^{40}K were included in the simulation. The manmade radionuclide ^{137}Cs was initially excluded, simply because the activity concentrations in the Mediterranean Sea are rather low.

2.2. External algorithms for the histogram calibration and convolution

The efficient reproduction of the actual spectrum from the simulated ones requires the detector energy resolution and the energy calibration to be precisely introduced. Both parameters are essential to the FSA calculations. As it has been reported in the past, any gain mismatch between the experimental and simulated spectra can greatly affect the results (Caciolli et al., 2012, van der Graaf et al., 2011). The utilized MC code offers the possibility to include these parameters in the simulation. Nevertheless, both the detector resolution and the behavior of the electronic components can vary from one measurement to the other. The inclusion of these parameters in the MC input file would lead to inefficient and time consuming repetitions.

Therefore a Gaussian broadening was externally applied in the obtained MC histograms, using an appropriate convolution algorithm as described by van der Graaf et al. (2011). The detector resolution can be determined either by using directly the experimental spectrum or by using standard reference sources. The energy resolution values were fitted by an arbitrary exponential function which was subsequently introduced in the algorithm to perform the Gaussian broadening. Moreover, the reproduction of the experimental binning and energy calibration was also externally achieved via a different algorithm in which the simulated spectra were reformed according to the experimental energy calibration of the spectrum, namely the calibration constant (keV/channel) and the energy offset (keV), assuming a linear energy function. The calibration of the MC spectra is a crucial step to the overall procedure in order to match the gain settings of the experimental spectrum, as gain mismatch can drastically affect the activity concentration results. Moreover, it is a necessary step before the minimization procedure, since both the experimental and the MC spectra are introduced as input (in counts per channels) in the MINUIT package. The algorithm can in principle incorporate the possibility of a non-linear rebinning of the MC spectra but the effect of such energy non-linearities in the experimental spectra were found to be negligible.

In Fig. 3 the steps of the described procedure are illustrated for the standard spectrum of the radionuclide ^{214}Bi. The normalized MC spectrum (after the multiplication with the effective volume and the acquisition time) assuming 1 Bq/l activity concentration is depicted in Fig. 3(a), along with the result of the implementation of the external convolution algorithm (Gaussian broadened spectrum), while the gain calibration procedure using the external rebinning algorithm is demonstrated in Fig. 3(b).

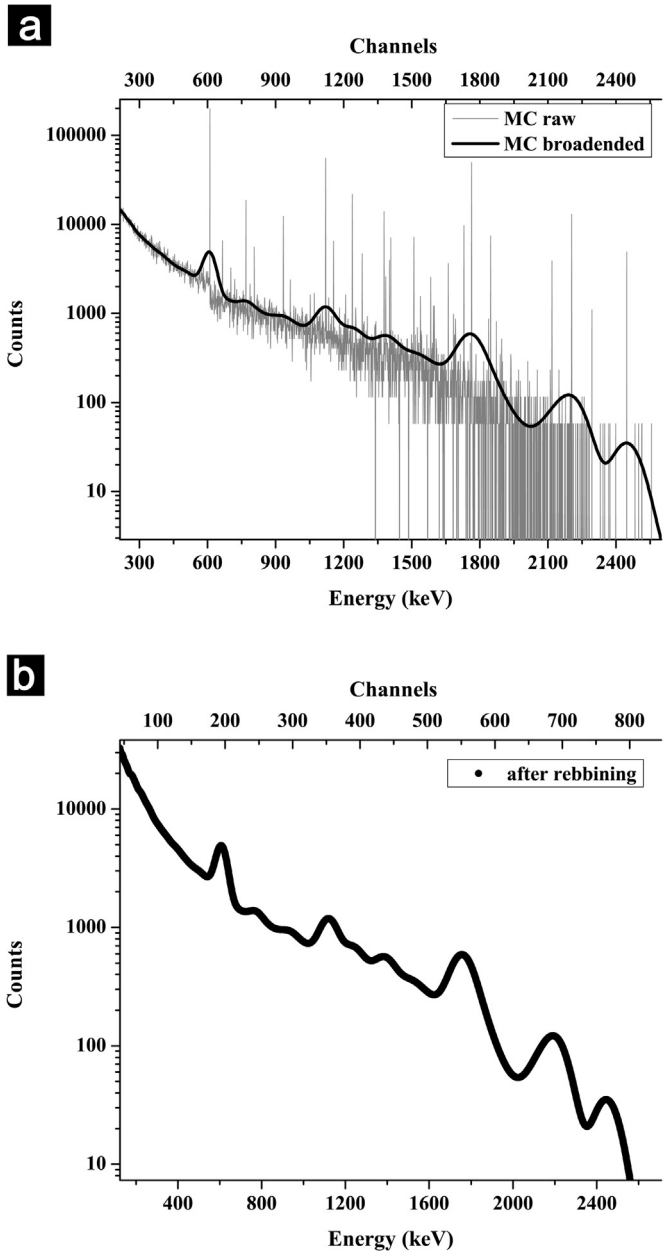

Fig. 3. Representation of the standard spectrum for the radionuclide ^{214}Bi in the three processing steps. The MC spectrum after the multiplication with the effective volume and the acquisition time (MC raw), assuming 1 Bq/l activity concentration, is depicted along with the corresponding spectrum after the implementation of the Gaussian broadening (MC broadened), in panel a, and after the rebinning procedure, in panel b.

2.3. Standard spectra

The final convoluted spectra implemented to simulate the marine environment consist of 10 separate spectra from the ^{238}U and ^{232}Th series along with ^{40}K. These spectra are presented in Fig. 4(a) for the radionuclides of the ^{232}Th series along with ^{40}K and in Fig. 4(b) for the radionuclides of the ^{238}U series, assuming a 1 Bq/l activity concentration for all the radionuclides and typical values for the electronic calibration (energy resolution and binning). The emitted γ-rays are reproduced according to the decay scheme for each radionuclide. In the case of ^{40}K, although only a single γ-ray at 1460.8 keV is emitted, additional features are present in the spectrum. These are artifacts attributed to low MC statistics in those areas. In Fig. 4(c), all the standard spectra

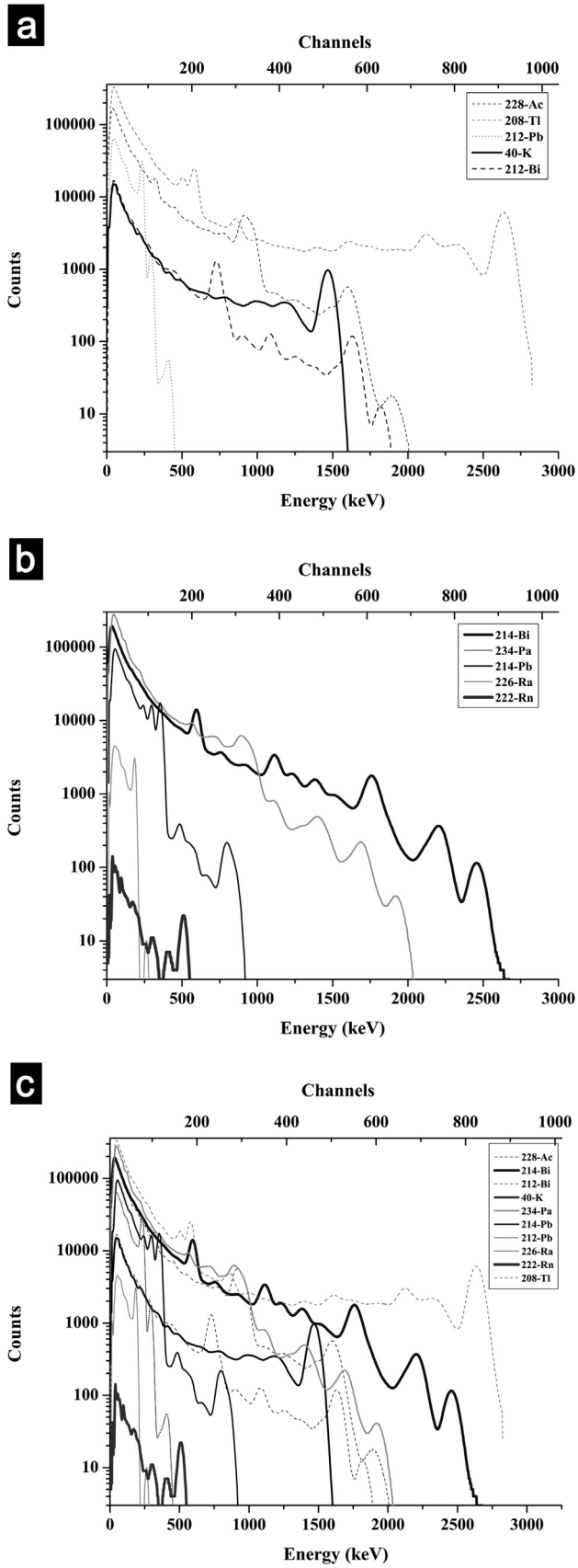

Fig. 4. Representation of the 10 standard spectra for the radionuclides ^{40}K and the ^{232}Th series (Fig. 4(a)) and the ^{238}U series (Fig. 4(b)), along with the total MC spectrum (Fig. 4(c)) assuming equal 1 Bq/l activity concentrations for all the radionuclides.

(assuming a 1 Bq/l activity concentration) are presented together. The MC spectra consist of many convoluted peaks in practically every energy region, due to the inherent low resolution of the employed detector (NaI(Tl) crystal).

More specifically, starting with the high energy part of the spectrum the first peak (at about 2600 keV) is a convolution of the ^{208}Tl (2614 keV with 99% intensity) and ^{214}Bi (2447.86 keV with 1.6% intensity) photopeaks, while the second one consists of the ^{208}Tl first escape peak (2103 keV), the ^{208}Tl Compton edge (2381 keV) and the ^{214}Bi photopeaks (most prominent one at 2204 keV with 5.1% intensity). Moving to the left (lower energy part) the complexity rises, as more radionuclides contribute to each peak formation. The peak present at 1760 keV is mostly attributed to the γ-rays of ^{214}Bi (at 1729 and 1765 keV) while a notable contribution arises to the left side from the ^{228}Ac photopeaks (1588 keV is the most prominent photopeak with 3.2% intensity) and from the ^{208}Tl second escape peak (1592 keV). Additional peaks with reduced contributions are the ^{234}Pa and ^{212}Bi ones, while several sum peaks could be hidden under the convoluted peaks due to the ^{214}Bi and ^{234}Pa complex cascade decay schemes (e.g. summation of the ^{214}Bi 609 and 1120 keV γ-rays). The ^{40}K photopeak (1461 keV), which is always present and usually predominant in spectra obtained in the seawater column, strongly interferes with the Compton edge of the 1764.5 γ-ray (1541 keV) and several ^{214}Bi photopeaks (most prominent at 1377 keV with 5.1% intensity) and much less with ^{234}Pa photopeaks (most prominent at 1394 keV with 2.1% intensity).

The complexity in the medium energy part of the spectrum rises due to the presence of many γ-rays from various radionuclides, while the situation is much improved in the lower energy part of the spectrum where the photopeaks of ^{214}Pb (241, 295, 352 keV) and ^{212}Pb (239 keV) are well separated from contributions originating from other radionuclides. The presented standard spectra were produced assuming an initial 1 Bq/l activity concentration and were subsequently utilized in the FSA calculations through χ^2 minimization.

2.4. The implementation of the χ^2 minimization

The key aspect of the FSA technique is the implementation of the χ^2 minimization in order to derive the optimal values for the unknown parameters under study. The estimation of the unknown parameters is accomplished by minimizing the difference between simulated and experimental data, with the former being represented by a collective function $F(\alpha_j)$, where α_j are the unknown normalization factors (James, 1994; James and Roos, 1975). Among the different minimization algorithms, the MINUIT package (developed at CERN by the CN/ASD Group, 1993), utilized in this work, is designed to handle any function F(X) offering the possibility to incorporate user-defined subroutines and has been successfully implemented in a great variety of different applications in the past.

In the present application a user-defined routine was developed and incorporated in the MINUIT package, to perform the minimization procedure and determine the optimal values of the unknown parameters α_j, which are in fact the activity concentrations. The minimization was performed according to the following reduced chi-square (χ^2) equation (James, 2004):

$$\chi^2=\frac{1}{N-M}\sum_{i=1}^{N}\left(ES_i-\sum_{j=1}^{M}\alpha_j MC_{ji}\right)^2$$

where:

i = the channel (up to N, usually equal to 1024 for standard NaI (Tl) scintillators).

M = the total number of standard radionuclide spectra (from j = 1 to 10 in the present case).

ESi = the measured experimental yield (counts) in channel i.

α_j = the activity concentration of each individual radionuclide, in units of Bq/l.

MC_{ji} = the yield of the final convoluted and rebinned MC spectrum of radionuclide j in channel i, in units of counts/(Bq/l).

It should be noted here, that in the marine environment, no 'background' spectrum or any other additional external contribution need to be subtracted. The contribution of the cosmic radiation to the Compton continuum in the experimental spectra is negligible, since the cosmic radiation is drastically decreased when the detector is placed at several meters below sea surface (Bagatelas et al., 2010; Androulakaki et al., 2015). The intrinsic radiation of the detection system is also negligible (Tsabaris et al., 2010). In fact, NaI(Tl) is one of the cleanest scintillators (Quarati et al., 2013), exhibiting small amounts (<0.5 ppm) of K in the crystal. This concentration contributes to the Compton continuum in the whole spectrum till 1.35 keV but the estimated count rate is extremely low ($\sim 10^{-3}$ counts/s/channel) as compared to the counting rate measured in the marine environment.

The minimization procedure, in more detail, is as follows: The calibration values (both energy and resolution) are provided by the user (operator) and then the external routines are executed to automatically derive the final standard spectra. The gain calibrated, broadened MC standard spectra (counts per channel) are introduced along with the experimental one in the MINUIT package. Then, the user-defined routine incorporated in the MINUIT package automatically performs a summation of the standard spectra by implementing a linear combination using different initial scaling factors (parameters) for each standard spectrum. Each factor αj, represents the activity concentration (in units of Bq/l) for the specific radionuclide. These unknown parameters are then automatically calculated using χ^2 minimization, to accurately fit the experimental spectrum. Therefore, the activity concentration results are directly obtained by the χ^2 minimization of the scaling parameters with respect to the experimental spectrum. The minimization is performed in steps using specific windows (channels), for which the number and the regions are selected by the user. These windows are not fixed and should be selected according to the experimental features of the spectrum, considering the inclusion of all the prominent peaks. The χ^2 minimization is then performed by calculating and comparing integrals in the selected regions (windows). Along with the experimental and simulated data (counts per channels), the user must provide the initial values and upper limits for the unknown parameters α_j which should be kept at positive and representative values according to the physical constraints of the problem. The control of unphysical results is handled by performing a biased chi-square minimization step by step in different selected windows starting from the high energy region (low count rates) and fixing the corresponding α_j values (for the radionuclides that contribute to the peak) in each step. The usage of many parameters α_j, and the performance of the minimization in steps, in properly selected regions of the spectrum, by fixing in each step the activity values of the corresponding radionuclides, increases the possibility of obtaining a unique 'more physical' solution. By performing the minimization in properly selected windows, the number of the available equations increases. Moreover, the number of the unknown parameters in each minimization step is decreased, since the photopeaks and the Compton continuum features are stored for the radionuclides contributing to the peaks of the selected window, by fixing the corresponding activity values. More importantly, the minimization procedure starts from the high energy region, which exhibits lower counting rates. In this way the minimization procedure is biased, focusing in these low statistics areas and forced to converge; thus the precision of the results is strengthened. Additionally, in the high energy part region the

presence of convoluted peaks is limited allowing for more reliable results. Moreover, a repetitive process to improve the accuracy of the obtained results was adopted, as described in detail in the following paragraphs. In the contrary case of using a single large minimization window (including all the spectral information), the minimization procedure would be mostly focused in the high count rate regions of the spectrum (low energy regions) and the convergence would be hindered by the high Compton continuum background interfering in these areas. The overall procedure is fast and the results are obtained in a few minutes, depending on the number of the α_j parameters and minimization windows. The activity concentration values are automatically printed in the screen in each step. The final output of the χ^2 minimization execution (apart from the printed activity concentration values) is the simulated spectrum with the activity concentrations incorporated.

Regardless the number of the utilized standard spectra (for different radionuclides) the FSA technique can give reliable results only for the radionuclides that contribute to the formation of a peak in the experimental spectrum. However, it can be implemented in order to estimate the Minimum Detectable Activity (MDA) values for any radionuclide. The accuracy of the results also strongly depends on the number of the utilized parameters and the minimization windows, since the minimization procedure is sensitive to the selection of such windows. In this work, the χ^2 minimization is performed in the selected energy windows (channels) stepwise, where each window includes one or several prominent peaks in the spectrum. The minimization procedure and the selected windows are schematically shown in Fig. 5, where the standard MC generated spectra for each radionuclide are given in typical activity concentration values found in the aquatic environment.

The starting point (i.e. the first minimization window) lies in the high energy region of the spectrum and is selected to be the energy interval under the first two peaks exhibiting the highest energy values (from approximately channel 650–990). The only radionuclides contributing to the formation of these peaks are ^{208}Tl and ^{214}Bi. By slightly changing the minimization window (3–4 channels) the best fit solution is obtained and therefore the activity concentrations for ^{208}Tl and ^{214}Bi, are fixed, allowing only for a slight variation around the obtained value (within ~5%) till the whole procedure converges. The remaining parameters (activity concentrations for the remaining radionuclides) are determined by repeating the same procedure after changing the minimization window, gradually moving towards the low energy part region, fixing in each minimization step the parameters of the corresponding radionuclides contributing to the existing peaks. The minimization procedure is completed when the last peak (that is, the peak with the lowest energy in the spectrum) is fitted.

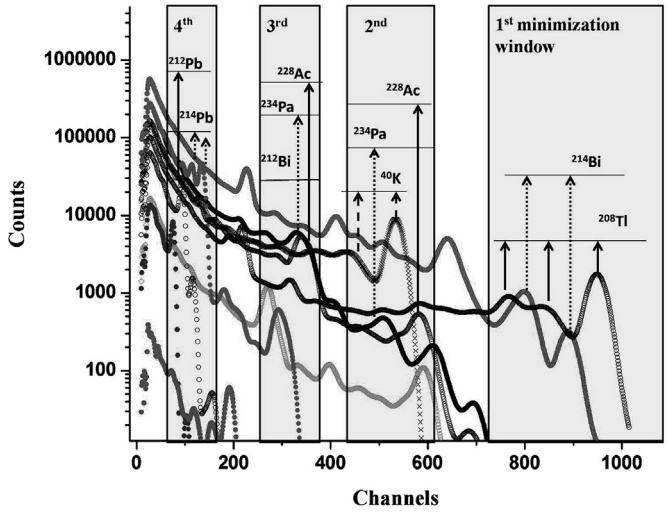

Fig. 5. Representation of the 10 standard spectra and the minimization windows assuming typical values for the activity concentrations of the radionuclides.

In more detail, as shown in Fig. 5, the next minimization window is selected to be around the peak at 1460 keV (^{40}K photopeak) including the first two peaks on the right (^{228}Ac γ-ray at 1588 keV, 510–570 channels) and left (^{40}K Compton edge, ^{214}Bi γ-ray at 1238 keV, 410–440 channels and ^{234}Pa γ-ray, 420–450 channels). In the third minimization window (220–343 channels) the activity concentration of ^{212}Bi (220–260 channels), ^{234}Pa (251–328 channels, most prominent peak at 934 keV) and ^{228}Ac (271–343 channels) are fixed, since the contribution in the selected area originates from the γ-rays of the aforementioned radionuclides and others that are already fixed (^{40}K, ^{214}Bi, ^{208}Tl). In the last (4th) minimization window, which includes the first three low-energy peaks in the spectrum (γ-rays from ^{214}Pb and ^{212}Pb), the parameters for ^{214}Pb and ^{212}Pb are fixed. Usually the photopeaks of ^{226}Ra (186 keV) and ^{222}Rn (511 keV) do not appear in the spectrum due to their low emission probabilities and high MDA values. In cases, however, where these peaks are evident in the experimental spectra, two additional minimization windows should be selected around the corresponding energy values. A schematic diagram of all the steps involved in the presented FSA technique, which does not necessarily require the *a priori* assumption of secular equilibrium is illustrated in Fig. 6.

Concerning the reliability of the utilized FSA technique, both statistical and systematic uncertainties are taken into account. The statistical uncertainty is estimated by taking into account the photopeak counting statistics of the experimental spectrum and the statistical uncertainty of the MC results. The statistical error in experimental yields typically ranges from 6% to 20% depending on the activity concentrations, the acquisition time and the γ-ray energy, while, regarding the MC simulations, the uncertainty was kept below 5% in the main photopeak regions for all the standard spectra. Thus the total statistical experimental uncertainty is mainly governed by the counting statistics. The systematic uncertainty on the other hand may be attributed to the simulation modeling (geometry measurement, materials), the energy and resolution calibration and to the minimization process (selection of the minimization windows). The systematic uncertainty arising from the selection of the minimization windows was estimated to be considerably less than 10% by changing the energy range of the selected windows. All the other contributions were considered as negligible, since these parameters were carefully tuned based on experimental data. Nevertheless, the systematic uncertainty critically depends on the accurate determination of the energy (gain) calibration, while possible miscalculations in the Gaussian broadening (energy resolution calibration) would mostly affect the fitting results and not the activity concentrations, since the minimization procedure is performed by count integration in the selected regions.

3. Implementation of the FSA technique in the laboratory

The FSA technique was applied to reproduce the results of the experimental calibration of the KATERINA detection system (Tsabaris et al., 2012a, 2012b, 2011, 2010, 2008) for measurements in the aquatic environment. The system KATERINA was deployed in a 5.5 m^3 water tank containing diluted sources of the radionuclides ^{40}K, ^{99m}Tc and ^{137}Cs having known activity concentrations (as shown in Table 1). Details on the experimental calibration procedure can be found elsewhere in the literature (Tsabaris et al., 2008; Vlastou et al., 2006). To reproduce the calibration spectrum, the

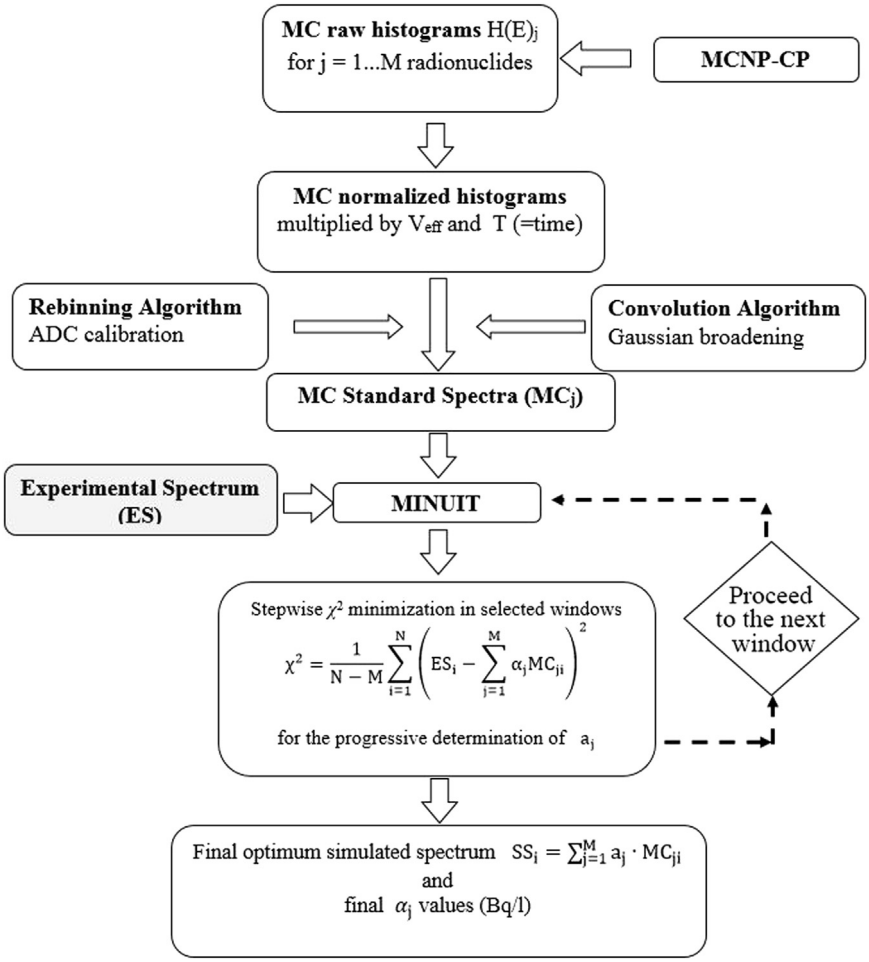

Fig. 6. Schematic of the steps involved in the adopted FSA technique from the MC simulations to the χ^2 minimization performance.

Table 1
Simulated and nominal activity concentration results (Bq/l) comparison for the calibration experiment using three (*first run*) and five (*second run*) standard spectra.

Radionuclides	*Nominal values*	First run		Second run	
		FSA (Bq/l)	%	*FSA* (Bq/l)	%
^{40}K	7.44	8.2	10	7.99	7
^{99m}Tc	4814	3900	23	3800	26
^{137}Cs	0.92	1.25	37	0.80	14
^{214}Bi	–	–	–	0.98	–
^{208}Tl	–	–	–	0.20	–

MCNP-CP code was implemented to simulate the three aforementioned radionuclides according to the exact existing experimental conditions. The three standard spectra (^{40}K, ^{99m}Tc and ^{137}Cs) were linearly combined to form the simulated spectrum. The theoretical activity concentrations were derived directly through χ^2 minimization, using the MINUIT package, by fitting the simulated spectrum to the experimental one. The experimental spectrum is depicted with the simulated one after the minimization procedure in Fig. 7(a).

The activity concentrations derived via the FSA technique are compared with the nominal ones in Table 1. It is evident that the reproduction of the experimental spectrum is poor (Fig. 7(a)) and the comparison of the activity values exhibits large differences, up to 40% for the radionuclide ^{99m}Tc (Table 1). This is attributed to the ambient background radiation (cosmic radiation, building materials) as well as to background contributions from the water constituents of the tank, which are not subtracted from the experimental spectrum. Moreover, the observed discrepancies at the low energy peak (the case of ^{99m}Tc) are attributed to pile-up effects that were present due to the high activity concentration of the ^{99m}Tc calibration source. The pile-up contribution in the experimental spectrum was calculated to 10%.

Therefore, the χ^2 minimization was repeated, after the inclusion in the calculations of two additional standard spectra (total of five), for the radionuclides ^{214}Bi and ^{208}Tl, since the corresponding photopeaks of these radionuclides were evident in the experimental spectrum (peaks at 609, 2200 and 2600 keV) yielding a significant contribution to the measurement. The 'corrected' simulated spectrum is compared with the experimental one, as shown in Fig. 7(b). The improvement in the results (Table 1) is reflected also in the better quality fitting of the experimental spectrum. The differences between the nominal and the FSA activity values were found to be ~7%, 14% and 26% for the radionuclides ^{40}K, ^{137}Cs and ^{99m}Tc, respectively. The enhanced difference found only in the case of the radionuclide ^{99m}Tc can be exclusively attributed to artifacts in the experimental measurement pile-up due to the high count rate, which were not corrected, nor included in the simulation.

An important result from this validation procedure was that the technique is highly sensitive to the complete representation of the simulated environment. A poor representation using a diminished number of standard spectra is directly reflected in the significant differences in the spectral features both in the photopeak regions, but also in the Compton continuum (Fig. 7(a)). However, when standard spectra from all the radionuclides that contribute to the

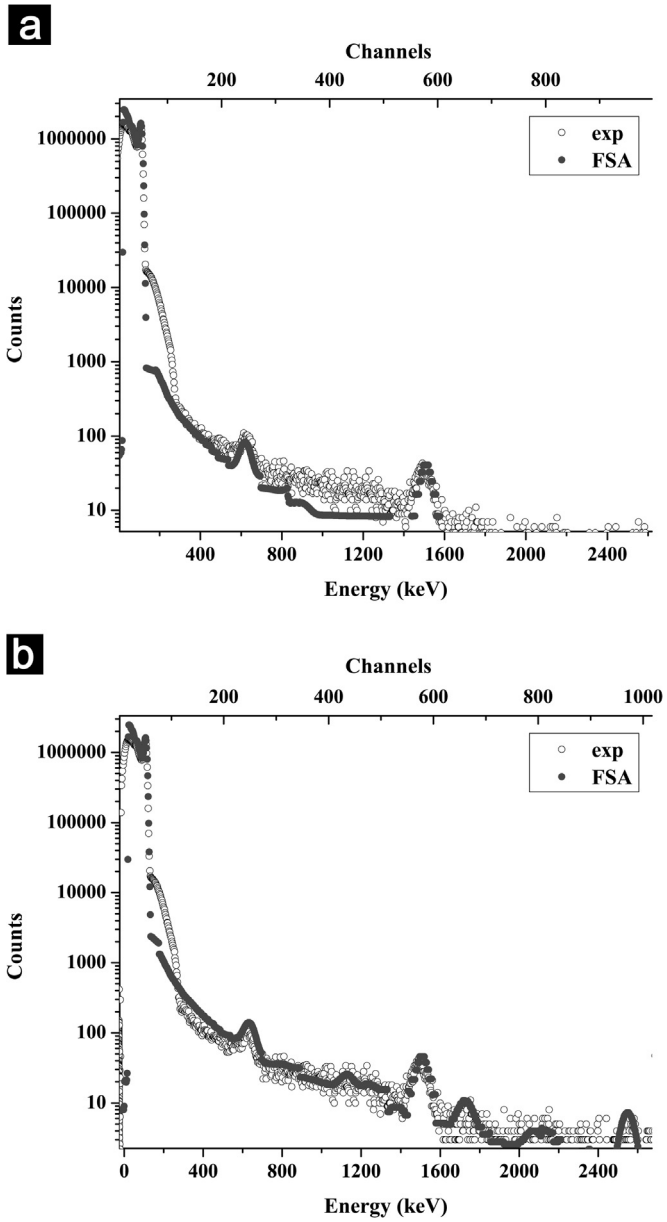

Fig. 7. Comparison between the simulated and experimental spectra of the water tank utilizing three standard spectra for the radionuclides ^{40}K, ^{137}Cs and ^{99m}Tc (panel a), and utilizing five standard spectra for the radionuclides ^{40}K, ^{137}Cs, ^{99m}Tc, ^{214}Bi and ^{208}Tl (panel b).

measurement are included in the calculations, the FSA results can accurately reproduce all the features of the experimental spectrum (Fig. 7(b)).

4. Applications in the marine environment

The method was tested in three marine environments exhibiting different activity concentrations for the studied radionuclides and different measurement setups (acquisition time, gain calibration). The measurements were held at Vasilikos port (Cyprus) (site1), Ierissos Gulf (Greece) (site 2) and Stoupa Bay (Greece) (site3). The FSA technique was applied in all cases and the results were compared with the activity concentrations derived by analyzing the experimental spectra (sites 1, 2 and 3) using the SPECTRW software (Kalfas, 2011). The discussed methodology was applied in all cases, while an additional FSA performance test was conducted in site 3, assuming secular equilibrium between the radionuclides of the same series. In this case only three standard spectra were utilized, namely the standard spectra from ^{40}K, ^{238}U (summation of the standard spectra from the radionuclides ^{214}Bi, ^{214}Pb, ^{234}Pa, ^{226}Ra and ^{222}Rn) and ^{232}Th (summation of the standard spectra from the radionuclides ^{208}Tl, ^{228}Ac, ^{212}Bi and ^{212}Pb).

4.1. Application in Vasilikos

The detection system KATERINA was deployed in Vasilikos port near a former fertilizer industry. The system was positioned well above the seabed and below the seawater surface and the experimental spectrum was obtained using a 17- hour acquisition time. Details for the area and the measurement setup are found at Androulakaki et al. (2015). The experimental spectrum was analyzed to determine the energy resolution (FWHM calibration), the energy calibration (gain setup) and the activity concentration values for ^{40}K and ^{214}Bi using the SPECTRW software. The activity concentration value for ^{40}K was determined by peak integration of the corresponding peak (at 1461 keV) and by subtracting the counts attributed to the ^{214}Bi photopeaks. The obtained values concerning the resolution and the energy calibration were properly fitted and introduced in the external algorithms to reproduce the standard spectra according to the measurement setup.

The experimental spectrum is compared with the theoretical one in Fig. 8. The reproduction of the Compton continuum and the peaks over the whole experimental spectrum is very satisfactory. The corresponding activity concentration values for the radionuclides ^{40}K and ^{214}Bi are compared with the experimental ones in Table 2 (site1). The relative differences from the experimental values for both radionuclides did not exceed 10%.

4.2. Application in Ierissos

The detection system KATERINA was deployed in the Ierissos port which is located in Chalkidiki near an operating gold mining industry. More details about the study area can be found at Pappa et al. (2013). The system was positioned well above the seabed and below the seawater surface and the experimental spectrum was obtained using a 9-hour acquisition time.

The experimental spectrum is presented along with the theoretical one in Fig. 9. The reproduction of the peaks appearing in the

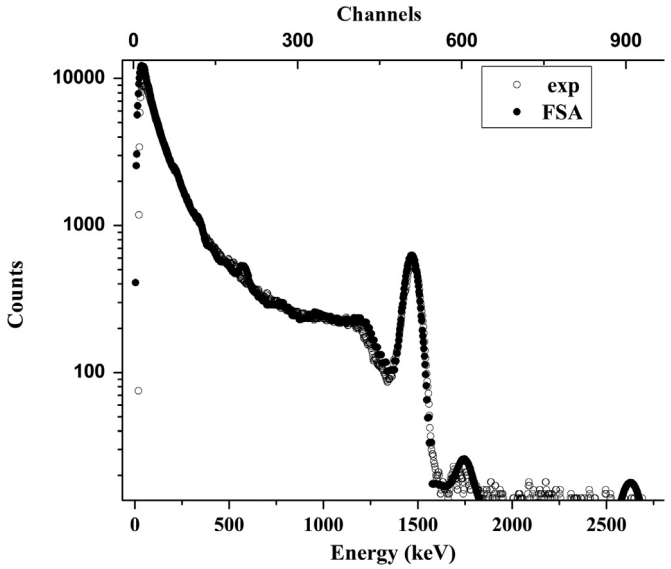

Fig. 8. Comparison between the simulated and experimental spectra for site1 (Cyprus).

Table 2
Simulated and experimental activity concentration results (Bq/l) for the two deployments, in Vasilikos port (site1) and in Ierissos Gulf (site2).

Sites	1			2		
Nuclides	*In situ* (Bq/l)	*FSA* (Bq/l)	%	*In situ* (Bq/l)	*FSA* (Bq/l)	%
^{40}K	18.1 (6%)	16.8	8	15.06 (8%)	13.85	9
^{214}Bi	0.26 (21%)	0.24	8	0.34 (19%)	0.31	10

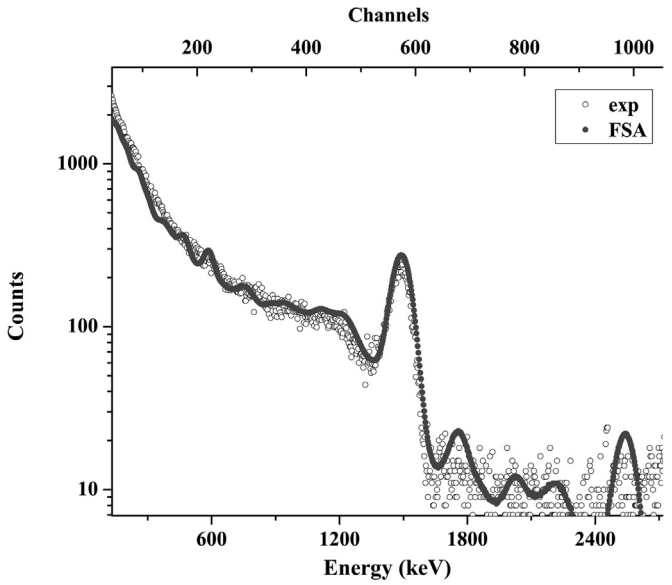

Fig. 9. Comparison between the simulated and experimental spectra for site2 (Ierissos Gulf).

experimental spectrum, along with the Compton continuum, is again satisfactory. The corresponding activity concentration values for the radionuclides ^{40}K and ^{214}Bi are compared with the experimental ones in Table 2 (site2). The relative differences from the experimental values for both radionuclides were found again to be around 10%.

4.3. Application in Stoupa

A dynamic environment where Submarine Groundwater Diffusion (SGD) sources (Burnett et al., 2006) were present, was additionally selected to apply the adopted methodology. In such environments, freshwater enters in the marine aquifer by diffusion through underground paths. The detection system KATERINA was deployed in the Kalogria Bay to acquire measurements in the water column in close touch with the SGD source. The Kalogria Bay is located north of Stoupa town, in the southwest Peloponnesus (Messinia Prefecture) and the area is characterized by the presence of numerous minor SGDs. The spectrometer KATERINA was deployed for several different periods, from July 2009 till May 2010. Details on the experimental setup are given in the literature (Tsabaris et al., 2012a). The experimental activity concentration values were derived by analyzing the *in situ* data as discussed above. Moreover, in order to check that all the radionuclides present in this environment were included in the FSA analysis, high resolution measurements by means of a HPGe system were performed on collected water samples from the site. These measurements yielded similar values with the *in situ* ones (Eleftheriou et al., 2013). The selected experimental spectrum for the application of the FSA technique was obtained during an expedition on March 2010. The minimization procedure was executed twice, first by simulating only three standard 'series' spectra, namely ^{40}K, ^{238}U and ^{232}Th, assuming secular equilibrium between the radionuclides of the same series, followed by a second analytical FSA performance test using 10 standard spectra, as discussed above. The first run was performed in order to investigate the validity of the secular equilibrium assumption.

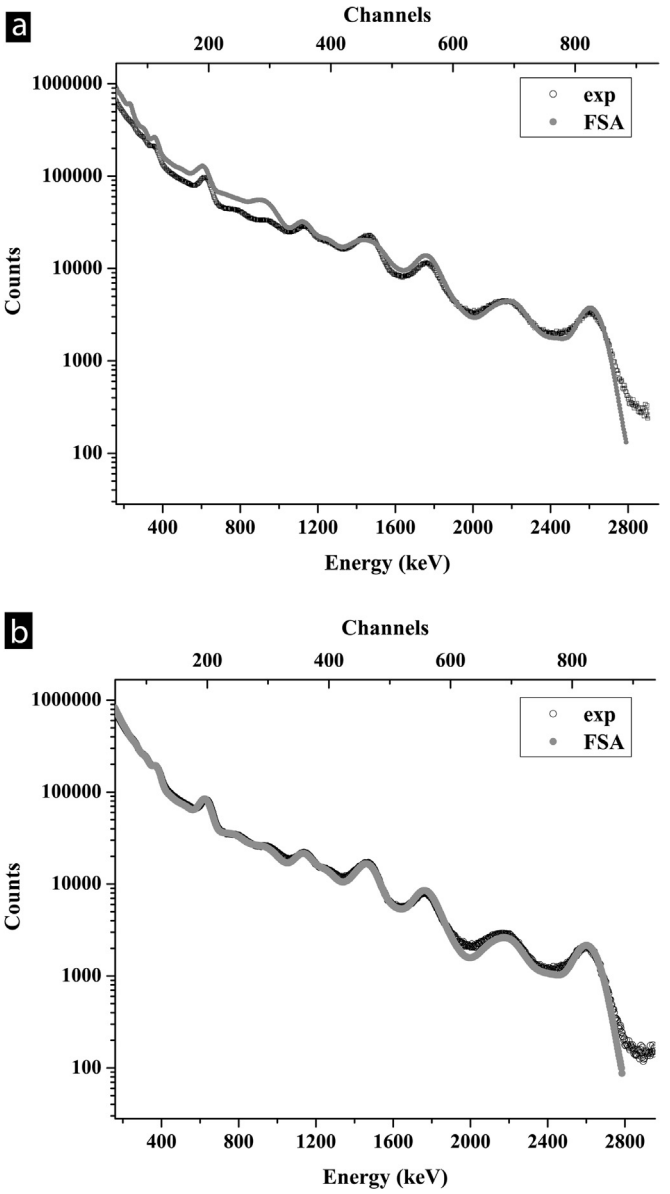

Fig. 10. Comparison between the simulated and experimental spectra for site3 (Stoupa Bay) using only three standard spectra for ^{40}K, ^{232}Th and ^{238}U assuming secular equilibrium between the radionuclides of the same series (10a) and using all 10 standard spectra (10b).

The experimental spectrum is presented along with the simulated ones in Fig. 10(a) (in the case of three standard 'series' spectra assuming secular equilibrium) and Fig. 10(b) (in the case of 10 standard spectra). The first run using the assumption of secular equilibrium among the radionuclides of the same series, failed to reproduce the experimental spectrum. This was expected, since the secular equilibrium is disturbed by the different solubility of the radionuclides in the water column. The differences between the two spectra are mostly attributed to the overestimation of the ^{234}Pa activity concentration (peak around channels 260–328) and ^{208}Tl as well as to the underestimation of ^{214}Bi. The effect in the corresponding estimated activity concentration values is significant, especially for ^{40}K (convoluted photopeak with ^{214}Bi, ^{234}Pa,

Table 3
Simulated (FSA) and experimental (*In situ*) activity concentration results (Bq/l) in Stoupa Bay (site3) using only three parameters considering secular equilibrium (1st run) among the radionuclides of the same series and using 10 independent parameters (2nd run).

Radionuclides	*In situ* (Bq/l)	1st run		2nd run	
		FSA (Bq/l)	%	*FSA* (Bq/l)	%
^{40}K	6.40 (6%)	10.38	62	7.02	10
^{214}Pb	3.27 (9%)	3.345	2	3.39	4
^{214}Bi	4.20 (5%)	3.345	20	4.30	2
^{208}Tl	0.30 (13%)	0.3547	18	0.32	7
^{228}Ac	1.05 (10%)	1.0641	1	1.2	14

^{228}Ac) as shown in Table 3 (1st run). The activity concentrations in the second run, were found to be in very good agreement with the experimental ones, as shown in Table 3 (2nd run).

5. Discussion and perspectives

A new approach for *in situ* quantitative measurements in the marine environment has been developed in cases where the low resolution of the γ-spectroscopy detector hinders the accurate determination of the activity concentrations. The activity concentration values were derived theoretically using the MCNP-CP code to simulate γ-ray spectra acquired in the seawater by a NaI (Tl) scintillation detector (system KATERINA) and the FSA technique.

The satisfactory reproduction of the experimental data renders the MCNP-CP code appropriate to be utilized in diverse environmental applications. The main advantages of the utilized MC code are the automatic consideration of the true coincidence summing effect in contact geometries and the direct simulation of all the prominent emitted γ-rays along with the corresponding intensities for each radionuclide.

The adopted methodology offers the possibility of rapid activity concentration calculations in any aquatic environment using detection systems based on NaI(Tl) crystals and could be easily readjusted to include different types of detectors (e.g. BGO, CeBr3, HPGe). The minimization is performed in selected windows covering the whole spectral range and the convergence is reached within a few minutes, provided that the electronic setup calibration is carefully matched to the experimental measurement, through the tuning of external algorithms.

The accuracy of the results depends initially on the accuracy of the MC spectra, therefore all the details of the experimental measurements affecting the results should be incorporated in the simulations. Assuming that a proper representation of the measurement is achieved (correct simulation of materials and inclusion of all the present radionuclides) two steps of the FSA procedure contribute to the overall uncertainty. These are the energy calibration and the proper selection of the various minimization windows, although the latter constitutes a less critical factor. The FSA technique is very sensitive to the energy calibration and any gain mismatch can greatly affect the activity concentration results. Therefore, a precise determination of the calibration constant and the offset is required for accurate results using the FSA technique, since these values are necessary for the rebinning procedure.

The method provides a unique solution yielding accurate results and it is sensitive to detect and identify anomalies that could be related to unexpected radionuclides, since the analysis comprises all the features of the spectrum. More importantly, there are features (escape peaks, Compton edges, sum peaks) present in the spectrum that often interfere with the photopeaks. When the spectrum is treated merely by window or peak analysis, these features cannot be quantified and experimentally subtracted, thus the analysis leads to a decrease in the accuracy of the obtained results. On the contrary, in the FSA technique these features are by definition included in the analysis and are properly taken into account automatically in order to estimate the activity results.

An interesting result from the experimental tests in the marine environment was the inadequacy of the *a priori* assumption concerning the existence of secular equilibrium to reproduce the experimental data. As demonstrated above, this assumption can greatly affect the quality of the theoretical spectrum as well as the activity concentration results and thus it should be avoided for marine environment applications.

The developed methodology concerns only naturally occurring radionuclides but it can be easily readjusted to include artificial radionuclides, for example the ^{137}Cs radionuclide, which can significantly contribute to the spectrum, depending on the area of the application. Moreover, the overall methodology does not depend on the specific geometry and the materials involved and thus, it can be applied for various geometries and different environments (seabed, soils), provided that accurate standard spectra exist for the geometry and/or materials under study.

Since the method has been successfully implemented in the aquatic environment, it will be subsequently implemented for seabed applications. To accurately reproduce the experimental spectra obtained on the seabed, it is mandatory to perform appropriate adjustments to the MC model according to the geometry set up for *in situ* measurements on the seabed and the physical characteristics of the source (sediment material).

A great advantage of the proposed methodology is that it can be implemented to derive MDA values for selected radionuclides (e.g. ^{137}Cs, ^{226}Ra) in every environment. Therefore, as a next step, an ongoing study is under way to derive the MDA values for ^{137}Cs, with respect to different salinity values, and thus ^{40}K activity concentrations.

Acknowledgments

The authors would like to acknowledge the BS-ERANET Project Partners and the support of the GSRT ESPA research program 12CHN212 'Research and development of an *in-situ* underwater gamma-ray spectrometer for low-level radioactivity measurements'. Moreover, one of the authors was partially supported by the program “Scholarships of IKY in the Marine and Inland Management of Water Resources” (Off.Gaz.:2850/B/22-10-2014, Contr. No:9) co-funded by EEA grants – Financial Mechanism 2009–2014 (85%) and the Hellenic General Secretariat for Investments and Development (15%). The authors would like also to thank Dr A. N. Berlizov for kindly providing the MCNP-CP code and Dr C. A. Kalfas for supporting the analysis of the γ-ray spectra by providing the software package SPECTRW.

References

Androulakaki, E.G., Tsabaris, C., Eleftheriou, G., Kokkoris, M., Patiris, D.L., Vlastou, R., 2015. Seabed radioactivity based on in situ measurements and Monte Carlo simulations. Appl. Radiat. Isot. 101, 83–92.

Bagatelas, C., Tsabaris, C., Kokkoris, M., Papadopoulos, C.T., Vlastou, R., 2010. Determination of marine gamma activity and study of the minimum detectable activity (MDA) in 4pi geometry based on Monte Carlo simulation. Environ. Monit. Assess. 165, 159–168.

Berger, M. J., Hubbell, J. H., Seltzer, S.M., Chang, J., Coursey, J.S., Sukumar, R., Zucker, D.S., Olsen, K., 2010. XCOM: Photon Cross Section Database.

Berlizov, A.N., van Belle, P., Zuleger, E., Ottmar, H., 2011. Experimental re-evaluation of the γ-ray energy and emission probability for the 159 keV transition in ^{238}U following the α-decay of ^{242}Pu. Appl. Radiat. Isot. 68, 1822–1831.

Berlizov, A.N., Mayer, K., 2010. Fast and accurate approach to γ-spectrum modeling: a validation study with a shielded/unshielded voluminous uranium sample. Appl. Radiat. Isot. 68, 1822–1831.

Berlizov, A.N., Solovyena, S.L., 2008. A dynamic library for calculating true-coincidence summing correction factors. J. Radioanal. Nucl. Chem. 276, 663–668.

Berlizov, A.N., 2006. MCNP-CP, a correlated particle radiation source extension of a general purpose Monte Carlo N-Particle transport code. In: Semkov, T.M., Pommé, S., Jerome, S.M. (Eds.), ACS Symposium Series 945. American Chemical Society, Washington DC, pp. 183–194.

Briesmeister, J.F., 1997. MCNP – a General Monte Carlo N-Particle Transport Code. Los Alamos National Laboratory Report, LA-12625-M.

Burnett, W.C., Aggarwal, P.K., Aureli, A., Bokuniewicz, H., Cable, J.E., Charette, M.A., Kontar, E., Krupa, S., Kulkarni, K.M., Loveless, A., Moore, W.S., Oberdorfer, J.A., Oliveira, J., Ozyurt, N., Povinec, P., Privitera, A.M.G., Rajar, R., Ramessur, R.T., Scholten, J., Stieglitz, T., Taniguchi, M., Turner, J.V., 2006. Quantifying submarine groundwater discharge in the coastal zone via multiple methods. Sci. Total Environ. 367, 498–543.

Caciolli, A., Baldoncini, M., Bezzon, G.P., Broggini, C., Buso, G.P., Callegari, I., Colonna, T., Fiorentini, G., Guastaldi, E., Mantovani, F., Massa, G., Menegazzo, R., Mou, L., Rossi Alvarez, C., Shyti, M., Zanon, A., Xhixha, G., 2012. A new FSA approach for *in situ* γ ray spectroscopy. Sci. Total Environ. 414, 639–645.

CN/ASD Group CERN,1993. MINUIT, Users Guide, nProgram Library D506.

Eleftheriou, G., Tsabaris, C., Androulakaki, E.G., Patiris, D.L., Kokkoris, M., Kalfas, C.A., Vlastou, R., 2013. Radioactivity measurements in the aquatic environment using *in-situ* and laboratory gamma-ray spectrometry. Appl. Radiat. Isot. 82, 268–278.

van der Graaf, E.R., Limburg, J., Koomans, R.L., Tijs, M., 2011. Monte Carlo based calibration of scintillation detectors for laboratory and in situ gamma ray measurements. J. Environ. Radioact. 102, 270–282.

Guillot, L., 2001. Extraction of full absorption peaks in airborne gamma-spectrometry by filteringtechniques coupled with a study of the derivatives. Comparison with the window method. J. Environ. Radioact. 53 (3), 381–398.

Hendriks, P.H.G.M., Maučec, M., de Meijer, R.J., 2001. MCNP modelling of scintillation-detector γ-ray spectra from natural radionuclides. Appl. Radiat. Isot. 57, 449–457.

Jäderström, J., Mueller, W.F., Attrashkevich, V., Adekola, A.S., 2015. True coincidence summing correction and mathematical efficiency modeling of a well detector. Nucl. Instrum. Methods A 784, 264–268.

James, F., 2004. MINUIT Tutorial, Function Minimization, (Reprinted from the Proceedings of the) 1972 CERN Computing and Data Processing School, Pertisau, Austria, 10–24 September 1972.

James, F., 1994. MINUIT Function Minimization and Error Analysis: Reference Manual Version 94. 1. CERN- D506.

James, F., Roos, M., 1975. Minuit-A system for function minimization and analysis of the parameter errors and correlations. Comput. Phys. Commun. 10, 343–367.

Jones, D.G., 2001. Development and application of marine gamma-ray measurements: a review. J. Environ. Radioact. 53, 313–333.

Kalfas, C. A., 2011. A modern spectroscopy software package. in: Proceedings of the 20th conference of the Hellenic Nuclear Physics Society, 27–28 May 2011, Athens, Greece.

Mahmood, H.S., Hoogmoed, W.B., van Hentel, E.J., 2013. Proximal gamma-ray spectroscopy to predict soil properties using windows and full-spectrum analysis methods. Sensors 13, 16263–16280.

Maučec, M., de Meijer, R.J., Rigollet, C., Hendriks, P.H.G.M., Jones, D.G., 2004. Detection of radioactive particles offshore by γ-ray spectrometry Part I: Monte Carlo assessment of detection depth limits. Nucl. Instrum. Methods 525, 593–609.

Minty, B.R.S., 1992. Airborne gamma-ray spectrometric background estimation using full spectrum analysis. Geophysics 57, 279–287.

Pappa, F.K., Tsabaris, C., Kaberi, H., Zeri, C., Androulakaki, E.G., Pashalidis, I., Ioannidou, A., Kokkoris, M., Eleftheriou, G., Patiris, D.L., Vlastou, R., 2013. Sediment pollution by radionuclides and toxic metals in the Ierissos Gulf, North Aegean Sea, Greece. in: Proceedings of the 22th conference of the Hellenic Nuclear Physics Society, 30 May − 1 June 2013, Athens, Greece, 148–152.

Povinec, P.P., Osvath, I., Comanducci, J.-F., 2008. Underwater gamma-ray spectrometry. In: Povinec, P.P. (Ed.), Analysis of Environmental Radionuclides. Radioactivity in the Environment Series. 11. Elsevier, Hungary, pp. 463–476.

Quarati, F.G.A., Dorenbos, P., van der Biezen, J., Owens, Alan, Selle, M., Parthier, L., Schotanus, P., 2013. Scintillation and detection characteristics of high-sensitivity CeBr3 gamma-ray spectrometers. Nucl. Instrum. Methods A 729, 596–604.

Szentmiklósi, L., Kis, Z., Belgya, T., Berlizov, A.N., 2013. On the design and installation of a Compton–suppressed HPGe spectrometer at the Budapest neutron-induced prompt gamma spectroscopy (NIPS) facility. J. Radioanal. Nucl. Chem. 298, 1605–1611.

Tsabaris, C., Patiris, D.L., Karageorgis, A.P., Eleftheriou, G., Papadopoulos, V.P., Georgopoulos, D., Papathanassiou, E., Povinec, P.P., 2012a. In-situ radionuclide characterization of a submarine groundwater discharge site at Kalogria Bay, Stoupa, Greece. J. Environ. Radioact. 108, 50–59.

Tsabaris, C., Evangeliou, N., Fillis-Tsirakis, E., Sotiropoulou, M., Patiris, D.L., Florou, H., 2012b. Distribution of natural radioactivity in sediment cores from Amvrakikos Gulf (Western Greece) as a part of IAEA's campaign in the Adriatic and Ionian Seas. Radiat. Prot. Dosim. 150 (4), 474–487.

Tsabaris, C., Patiris, D.L., Lykousis, V., 2011. KATERINA: an *in situ* spectrometer for continuous monitoring of radon daughters in aquatic environment. Nucl. Instrum. Methods A 626–627, S142–S144.

Tsabaris, C., Scholten, J., Karageorgis, A.P., Comanducci, J.-F., Georgopoulos, D., Liong Wee Kwong, L., Patiris, D.L., Papathanassiou, E., 2010. Underwater *in situ* measurements of radionuclides in selected submarine groundwater springs, Mediterranean Sea. Radiat. Prot. Dosim. 142 (2–4), 273–281.

Tsabaris, C., Bagatelas, C., Dakladas Th, Papadopoulos, C.T., Vlastou, R., Chronis, G.T., 2008. An autonomous *in situ* detection system for radioactivity measurements in the marine environment. Appl. Radiat. Isot. 66, 1419–1426.

Vlastou, R., NtziouI, Th., Kokkoris, M., Papadopoulos, C.T., Tsabaris, C., 2006. Monte Carlo simulation of g-ray spectra from natural radionuclides recorded by a NaI detector in the marine environment. Appl. Radiat. Isot. 64, 116–123.

Wang, Y., Zhang, Y., Wu, N., Wu B., Liu, Y., Cao, X., Wang, Q., 2015. Monte Carlo Simulation of *in situ* Gamma-Spectra Recorded by NaI (Tl) Detector in the Marine Environment. J. Ocean Univ. China.

X-5 Monte Carlo Team, 2003. MCNP5 – A General Monte Carlo N-Particle Transport Code, Version 5. LA-UR-03–198, LA-CP-03–0245, Los Alamos National Laboratory.

Zhang, Y., Li, C., Liu, D., Zhang, Y., Liu, Y., 2015. Monte Carlo simulation of a NaI(Tl) detector for *in situ* radioactivity measurements in the marine environment. Appl. Radiat. Isot. 98, 44–48.

Zhu, H., Venkataraman, R., Menaa, N., Croft, S., Berlizov, A., 2008. Validation of gamma-ray true coincidence summing effects modeled by the Monte Carlo code MCNP-CP. J. Radioanal. Nucl. Chem. 278, 359–363.